Flow and Mixture Formation of a Fuel Spray impinging on a Wall – Experimental Studies and Numerical Simulation

Schittkowski T., Hildenbrand S., Staudacher S., Brüggemann D.[1]

1. LTTT, Universität Bayreuth, 95440 Bayreuth, Germany

A stationary spray chamber in combination with a Particle Image Velocimetry (PIV) system is used to study the interactions between a fuel spray impinging on a wall. Using this technique, 2-dimensional images of the velocity field of the gas and liquid flows are obtained.
Numerical simulation of the spray provides an opportunity for direct comparison of the experimental data with numerical results. Combining both methods allows for an immediate interaction between them and, as a consequence, for more accurate numerical simulations and experimental studies. The computations are carried out by a three-dimensional finite-volume computer code, using the Eulerian-Lagrangian approach for the continuous and the dispersed phase, respectively. In the CFD code standard models are implemented accounting for atomization, turbulence and impingement.

1. Introduction

In DI engines the interaction of the fuel spray with the chamber walls has a large influence on fuel dispersion, evaporation, mixture formation and combustion. The relevance of this effect has grown in the last years due to the development of small, high-speed direct injection engines, where the spray impinges on the piston in a short distance from the injector. A better understanding of this process could lead to further optimization of the combustion and minimization of emissions of soot and hydrocarbons.
Other groups concentrated on the internal spray structure [1, 2]; in our case the vortices that build up after the impact of the spray on the wall are of special interest. Other methods for the experimental analysis of sprays include Raman spectroscopy, high-speed PIV [3], phase sensitive PIV [4], Mie scattering for determination of droplet sizes and fluorescence techniques (LIEF) for structure analysis [5].

2. Computational method

The numerical simulations in this case have been performed by a three-dimensional finite volume computer program. Because of the transient behavior of spray computations, great emphasis is placed on the intermediate solutions of the simulation. Therefore, higher-order methods for both temporal and spatial discretization have been employed. In terms of temporal accuracy a second-order Crank-Nicholson scheme has been used and a second order monotone advection and reconstruction scheme (MARS) has been employed for spatial discretization. The discretized equations are then solved by the PISO algorithm [6], a non-iterative predictor-corrector method which is a commonly used means for solving fluid flow problems.

The gas phase is represented by a continuum and the governing equations (conservation of mass, momentum and energy) are expressed in Eulerian form. The dispersed phase is modeled in the Lagrangian framework with each droplet parcel being tracked separately. The droplet parcels consist of a statistically representative number of droplets with identical properties. Interaction between the two phases takes place by using source terms in the respective formulation of the employed equation. Turbulence is described by the standard k–ϵ model, which is used without wall-functions. This requires a fine mesh resolution up to the wall what entails increased computational time, but on the other hand a more accurately captured motion of the background fluid induced by the spray-wall interaction. Another problem in the near-wall area poses the so-called void fraction, i.e., the ratio of droplet volume to cell volume containing it. The Lagrangian model employed here bases on a point-volume approximation and therefore the volume fraction is very small. Due to the clustered cells near the wall, this ratio tends to be larger. However, no violation of the computational approach was encountered in the present calculations.

The computational domain used for this simulation is of cylindrical shape with physical dimensions of $r = 80\,\mathrm{mm}$ and $h = 50\,\mathrm{mm}$ for the radius and the height, respectively. The injector is placed at a height of 45 mm according to the experiment. The cylinder is numerically represented by a butterfly grid. In the internal part of the domain 50×50 grid points are used in $x-$ and $z-$ direction, the four domains surrounding this part each have 50×25 grid points. In the wall-normal direction 50 computational cells are used. Cell clustering has been employed in the $y-$direction in the vicinity of the bottom wall to comply with the requirements of the turbulence model (i.e., $y^+ \approx 1$).

Simulations have been carried out with air as background fluid at environmental conditions ($p_0 = 1\,\mathrm{bar}$, $T_0 = 300\,\mathrm{K}$). Dodecane has been chosen as injected fluid with temperature-dependant properties.

All computations have been performed with wall boundary conditions at the bottom and at the top of the domain, pressure boundaries have been set at the circumferential boundaries. An additional scalar transport equation for the evaporated liquid is solved. Droplet breakup due to aerodynamic forces is accounted for by the model of Reitz & Diwakar [7], spray-wall interaction is simulated with the wall-impingement model by Bai [8]. This model differentiates between three impingement regimes, namely rebound, spread and splash. The transition criteria are based on the droplet Weber number (ratio of droplet kinetic energy to surface energy) and on the droplet Laplace number (ratio of surface tension to viscous forces).

The pintle-type injector with model number *0 280 150 044* (by Bosch) has been modelled with a cross-sectional area of $2\,\mathrm{mm}^2$, a flow rate of $\dot{V} = 9.2 \cdot 10^{-6}\,{}^{\mathrm{m}^3}\!/\!_{\mathrm{s}}$ and an initial droplet size of $D_i = 60\,\mu\mathrm{m}$. A total of $46\,\mathrm{mm}^3$ has been introduced following the injection schedule shown in figure 1.

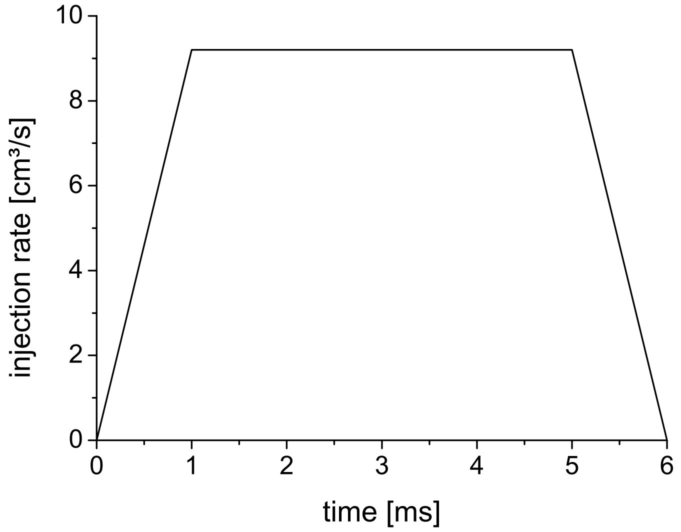

Fig. 1: Injection schedule

The injection pressure is $p_{inj} = 10\,\mathrm{bar}$, atomization of the liquid fuel entering the chamber is being accounted for by the model of Reitz & Diwakar [7]. The average injection velocity is $\bar{v}_{inj} = 38\,{}^{\mathrm{m}}\!/\!_{\mathrm{s}}$, which is consistent with the data measured in the experiment. For the present calculations, a parcel injection rate of $1 \cdot 10^6\,{}^{1}\!/\!_{\mathrm{s}}$ has been chosen. A time step of $\Delta t = 20\,\mu\mathrm{s}$ has been used.

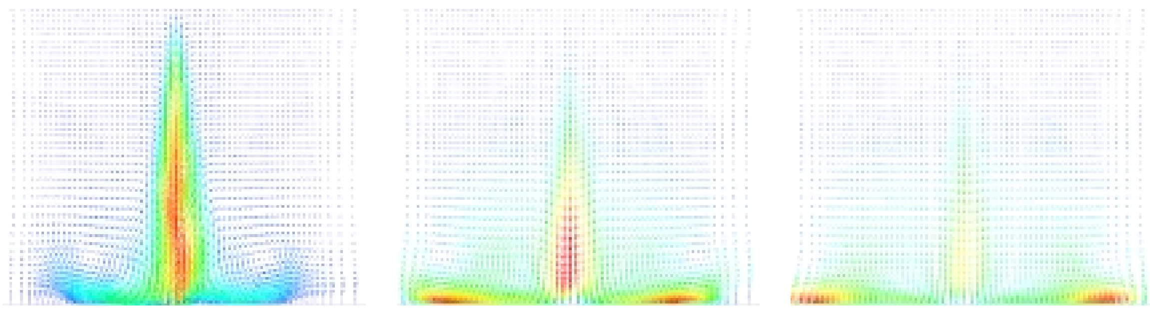

Fig. 2: Simulation results: velocity vectors after 5, 8 and 10 ms in the $z = 0$ level

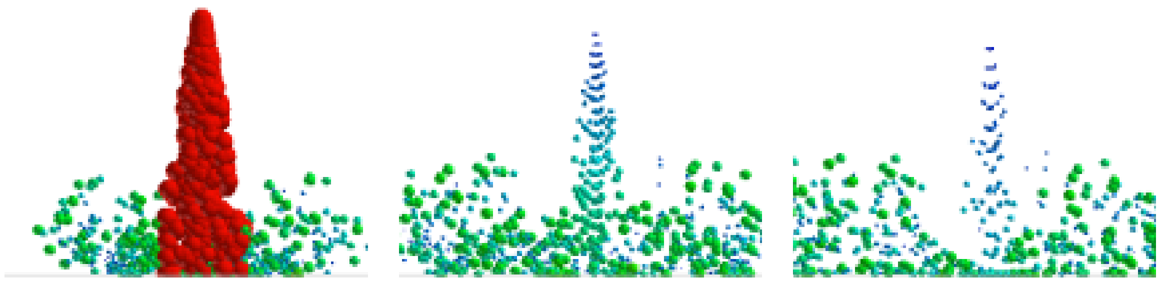

Fig. 3: Simulation results: droplet parcels after 5, 8 and 10 ms between $z = -1$ mm and $z = +1$ mm. The size of the parcels reflect the droplet mass.

3. Experimental setup

One of the problems encountered in the conduction of fluid-dynamic experiments is the non-intrusive determination of the velocity components in the flow. If the velocity vectors have to be determined spatially and temporally resolved, the technique of Particle Image Velocimetry (PIV), which has been developed 15 years ago and has been continuously enhanced since, offers a proper solution.

In this technique, the spatial offset of – available or added – particles between two laser pulses is measured; from the image containing these distances and the known pulse interval the two-dimensional velocity field is calculated.

We use a commercial PIV system from *LaVision* (FlowMaster) with two frequency-doubled NdYAG lasers, whose laser beams are combined to form the desired light sheet. The maximum power of each laser is 50 mJ per pulse. The double-frame CCD camera has an optical resolution of $1280 \cdot 1024$ pixel, a dynamic range of 12 bit and a maximum frame rate of 15 pictures per second. The light sheet formed by the lasers has a height of about 8 cm and a width at the waist of 0.5 mm.

The spray chamber used for these experiments is designed for maximum variability in terms of the spray parameters. A free spray over a length of 20 cm can be examined as well as a spray impinging on a surface. This copper surface has a distance of 5 cm from the spray nozzle and the angle can be varied to simulate different spray situations.

Within the chamber the parameters gas pressure (up to 40 bar), gas temperature (up to 550 K), spray temperature, injection pressure, wall temperature and the distance and angle between injector and wall can be varied. The impinging area can be heated independently from the chamber volume. Figure 4 shows the experimental setup in top view.

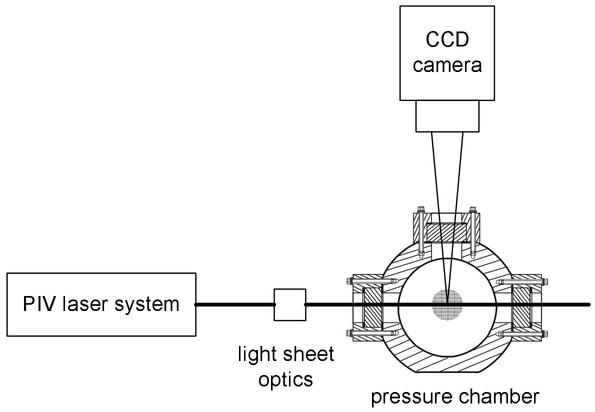

Fig. 4: Experimental setup for the PIV experiment

4. Experimental results

Depending on the chosen parameters for injection pressure p_{inj} and injection duration t_{inj}, the creation of vortices after wall impingement can be observed as seen in figure 5.

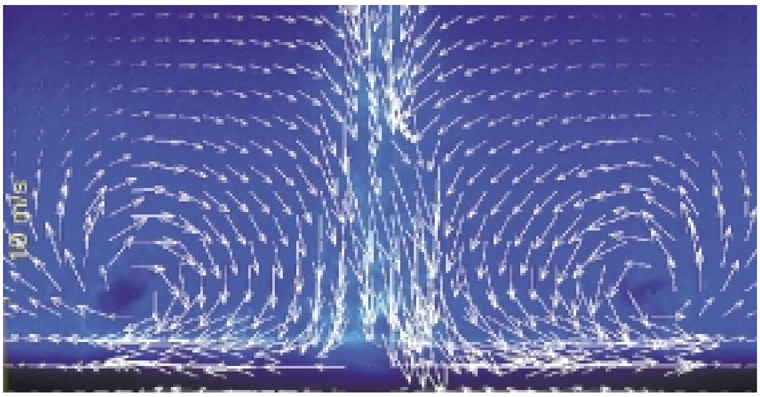

Fig. 5: Vortices within a spray impinging on a wall, obtained by PIV measurements

Figure 6 shows a comparison between the maximum spray radius at the end of the spray or at the wall, respectively. The values obtained from the images of the spray at the different time values are directly compared with the values obtained by numerical simulation.

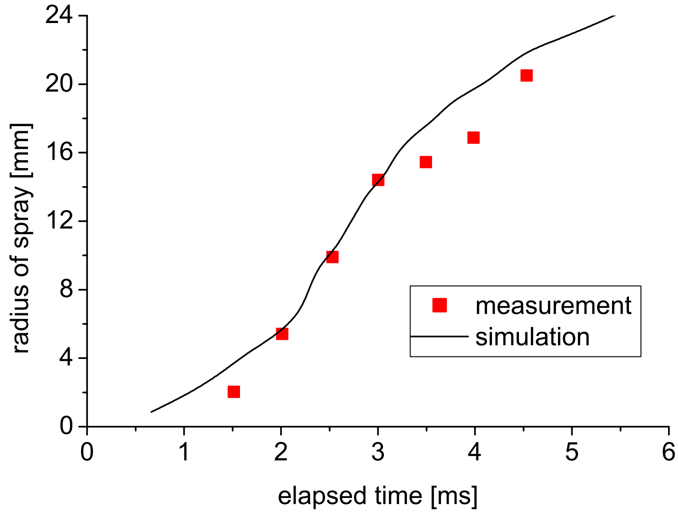

Fig. 6: Comparison of the maximum spray radius between measurement and simulation

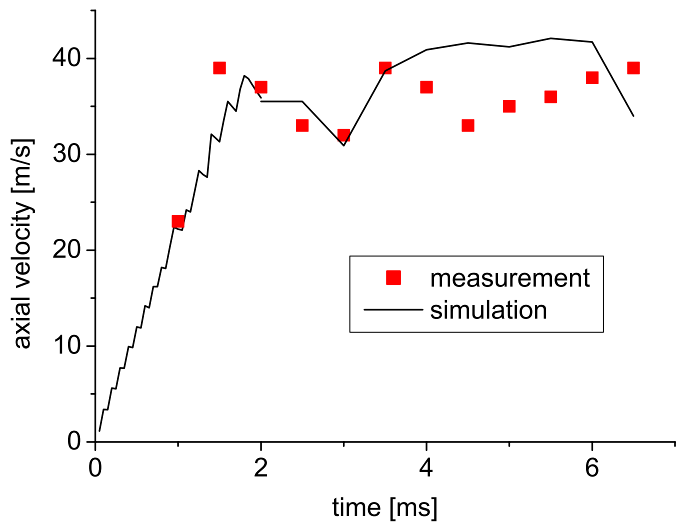

Fig. 7: Measured and simulated spray velocities of the spray tip (below 2 ms) and 5 mm above the surface (after 2 ms).

In figure 7 the measured spray velocities and the simulated spray velocities are compared. During the first 2 ms, before the spray impinges on the wall, the axial velocity of the leading spray particles is measured. After impingement, the spray velocity at a central position 5 mm above the wall is shown. In the beginning, the velocity increases due to the growing injection rate (as shown in figure 1), after reaching a maximum spray velocity of about 40 $^{m}/_{s}$, the speed of the spray particles remains constant until the velocity drops again because the end of the injection duration is reached (not shown in the graph).
The temporal evolution of the spray is shown in figure 8, where the dispersion of the spray is shown in combination with the corresponding velocity vectors. These images can be directly compared with the images obtained by numerical simulation shown in figure 3.

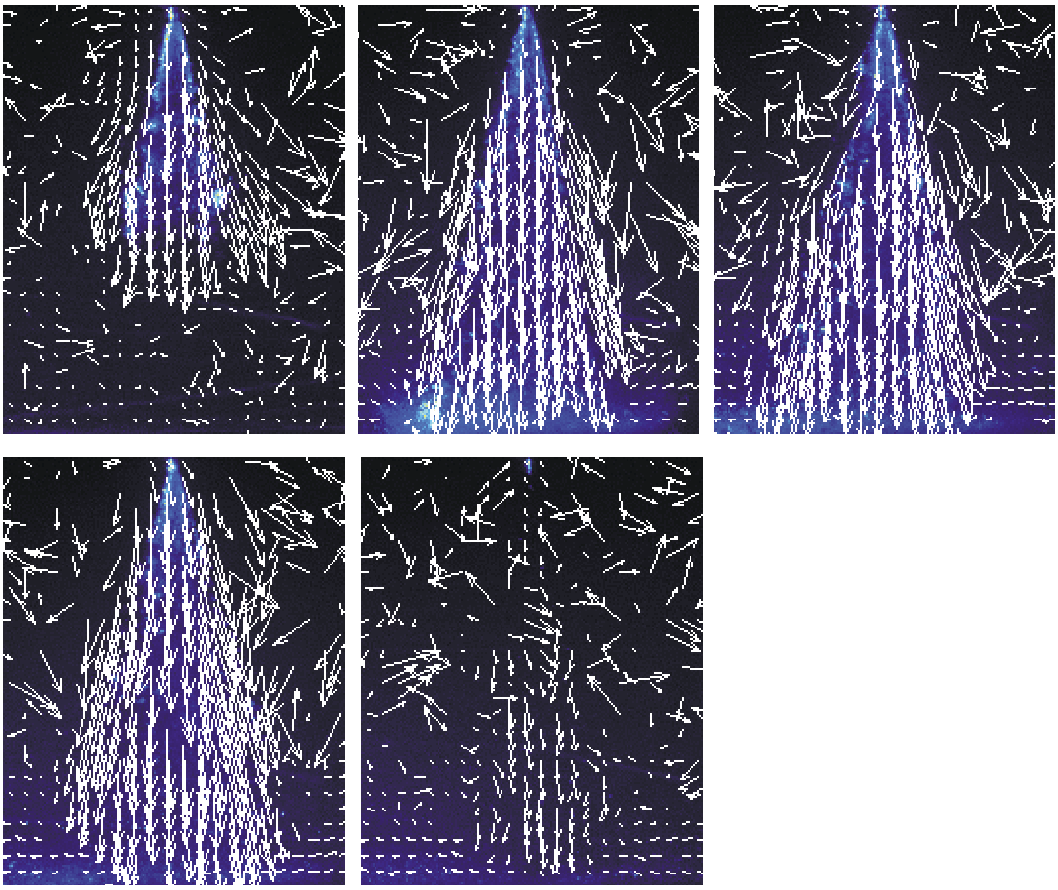

Fig. 8: PIV measurements of the spray after 2, 4, 6, 8 and 10 ms after start of the injection. The dimensions of the images are 40 mm width and 50 mm height.

5. Conclusion

A model spray has been numerically simulated and studied with an optical method for velocity determination and spray visualization. It is possible to compare directly the visualization of the droplet particles and the velocities of the spray and the surrounding air. A good agreement has been observed on some key parameters of the spray. A better approximation of the injection schedule to the experiment along with enhanced initial boundary conditions and atomization models could improve the results obtained in the simulation.

6. Acknowledgements

Financial support from the Bavarian research cooperation on turbulent combustion (FORTVER) is gratefully acknowledged.

References

[1] Cao Z-M, Nishino K, Mizuno S and Torii K 2000 *Experiments in Fluids* **29** 211–219

[2] Fujimoto H, Tanaka T, Ashida K, Yeom J-K and Senda J 2000 *10th International Symposium on Applications of Laser Techniques to Fluid Mechanics*

[3] Richter B, Rottenkolber G, Hehle M, Dullenkopf K and Wittig S 2001 *ILASS Europe*

[4] Rottenkolber G, Gindele J, Raposo J, Dullenkopf K, Hentschel W, Wittig S, Spicher U and Merzkirch W 1999 *PIV conference*

[5] Ipp W, Wagner V, Krämer H, Wensing M, Leipertz A, Arndt A and Jain A K 1999 *SAE* 1999-01-0498

[6] Issa R I 1986 *J. Comp. Phys.* **62** 40–65

[7] Reitz R D and Diwakar R 1986 *SAE* 860469

[8] Bai C and Gosman A D 1995 *SAE* 950283